

Research Article

Laser Irradiation Alters the Expression Profile of Genes Involved in the Extracellular Matrix *In Vitro*

Sandra M. Ayuk, Nicolette N. Houreld, and Heidi Abrahamse

Laser Research Centre, Faculty of Health Sciences, University of Johannesburg, P.O. Box 17011, Doornfontein 2028, South Africa

Correspondence should be addressed to Heidi Abrahamse; habrahamse@uj.ac.za

Received 16 April 2014; Accepted 25 May 2014; Published 23 June 2014

Academic Editor: Gerhard Litscher

Copyright © 2014 Sandra M. Ayuk et al. This is an open access article distributed under the Creative Commons Attribution License, which permits unrestricted use, distribution, and reproduction in any medium, provided the original work is properly cited.

The extracellular matrix (ECM) forms the basis of every phase in wound healing. Healing may be impaired if some of these components are destroyed. Photobiostimulation has demonstrated a stimulatory response in biological processes. This study aimed to evaluate various genes involved in the ECM, in response to laser irradiation. Isolated human skin fibroblasts were used in three different cell models, namely, normal, normal wounded, and diabetic wounded. Cells were irradiated with 5 J/cm² using a continuous wave diode laser emitting at a wavelength of 660 nm and incubated for 48 h. Nonirradiated (0 J/cm²) normal and diabetic wounded cells served as the control. Real-time reverse transcription (RT) quantitative polymerase chain reaction (qPCR) was used to determine the expression of 84 genes in a PCR array. There was a significant upregulation of 29 genes in the normal cells, 32 genes in the normal wounded cells, and 18 genes in the diabetic wounded cells as well as a downregulation of 19 genes (normal), 6 genes (normal wounded), and 31 genes (diabetic wounded). Low intensity laser irradiation (LILI) stimulates gene expression in various cell adhesion molecules (CAMs) and extracellular proteins at 660 nm in wounded fibroblasts *in vitro*.

1. Introduction

Components of the extracellular matrix (ECM) have been shown to be useful in wound healing [1, 2]. They form the core of every wound healing phase, and healing may be impaired if any of these components is destroyed [3]. In addition, they play a role in angiogenesis, tissue remodelling, and rapid scaffold breakdown [4]. The interaction between the ECM and various cells is very important for proper functioning of the cell [5–8]. This interaction could be direct or indirect. Directly, cellular receptors stimulate the ECM or indirectly, through the structural components of the ECM produced by glycoproteins. Cellular activities directed by these interactions are required for wound healing.

Regulation of the wound healing process comprises the interaction of various cell types, namely, neutrophils, lymphocytes, macrophages, and fibroblasts, and regular mediators such as growth factors and cytokines and ECM components (fibronectin (FN); fibrin; collagen; and elastin (EI)); laminin (LMN); proteoglycans (PG); glycosaminoglycans (GAG); matrix metalloproteinases (MMPs); and tissue inhibitor of metalloproteinases (TIMPs) [2].

For proper cell survival and gene expression in normal wound healing, the environment needs to be at equilibrium with the activity of growth factors, fibroblast interaction, and mechanical forces to ensure normal tissue remodelling [9]. Fibroblasts produce most of the molecules in the ECM including proteases, integrins, cytokines, and growth factors during tissue repair which are responsible for late phase tissue remodelling and eventually scarring [10, 11]. However, the situation is different in chronic wounds due to the disruption of the regular healing process because of tissue damage, biochemical and cellular imbalances, or an underlying pathological state such as diabetes and venous insufficiency. Venous leg ulcers (VLUs) are amongst the major problems in public health and have become an economic burden in most health care services. It is commonly associated with pain, reduces the quality of life, and is even associated with death. It may also cause tiredness and depression [12–14]. The prevalence of diabetic foot ulcers is approximately 1–2% worldwide [15]; it occurs at any age [16] with an incidence of 3–5% over 65 years [17].

Photobiostimulation, or photobiomodulation, is a non-invasive type of treatment that modulates the treatment of

TABLE 1: Laser parameters.

Laser parameters	
Wavelength (nm)	660
Wave emission	Continuous wave
Power output (mW)	92.5
Spot size (cm ²)	9.1
Output density (mW/cm ²)	10.22
Irradiation duration	8 min 9 s
Fluence (J/cm ²)	5

TABLE 2: Functional genes of the ECM and its adhesion molecules.

Pathway	Genes
Cell adhesion molecules	
Transmembrane molecules	CD44, CDH1, HAS1, ICAM1, ITGA1, ITGA2, ITGA3, ITGA4, ITGA5, ITGA6, ITGA7, ITGA8, ITGAL, ITGAM, ITGAV, ITGB1, ITGB2, ITGB3, ITGB4, ITGB5, MMP14, MMP15, MMP16, NCAM1, PECAM1, SELE, SELL, SELP, SGCE, SPG7, and VCAM1
Cell-cell adhesion	CD44, CDH1, COL11A1, COL14A1, COL6A2, CTNND1, ICAM1, ITGA8, and VCAM1
Cell-matrix adhesion	ADAMTS13, CD44, ITGA1, ITGA2, ITGA3, ITGA4, ITGA5, ITGA6, ITGA7, ITGA8, ITGAL, ITGAM, ITGAV, ITGB1, ITGB2, ITGB3, ITGB4, ITGB5, SGCE, SPP1, and THBS3
Other adhesion molecules	CNTN1, COL12A1, COL15A1, COL16A1, COL5A1, COL6A1, COL7A1, COL8A1, VCAN, CTGF, CTNNA1, CTNNB1, CTNND2, FN1, KALI, LAMA1, LAMA2, LAMA3, LAMBI, LAMB3, LAMCI, THBS1, THBS2, CLEC3B, TNC, and VTN
Extracellular matrix proteins	
Basement membrane constituents	COL4A2, COL7A1, LAMA1, LAMA2, LAMA3, LAMBI, LAMB3, LAMCI, and SPARC
Collagens and ECM structural constituents	COL11A1, COL12A1, COL14A1, COL15A1, COL16A1, COL1A1, COL4A2, COL5A1, COL6A1, COL6A2, COL7A1, COL8A1, FN1, and KALI
ECM proteases	ADAMTS1, ADAMTS13, ADAMTS8, MMP1, MMP10, MMP11, MMP12, MMP13, MMP14, MMP15, MMP16, MMP2, MMP3, MMP7, MMP8, MMP9, SPG7, and TIMP1
ECM protease inhibitors	COL7A1, KALI, THBS1, TIMP1, TIMP2, and TIMP3
Other ECM molecules	VCAN, CTGF, ECM1, HAS1, SPP1, TGFBI, THBS2, THBS3, CLEC3B, TNC, and VTN

wounds through various cellular or biological processes. It is effective in the visible and near infrared (NIR) spectral range. It functions at wavelengths of 500–1100 nm and a power output of 10–200 mW [18]. The use of photobiomodulation in wound healing has greatly ameliorated various cellular processes affecting different phases of wound healing. Studies have demonstrated the stimulatory effects of photobiomodulation in wounded cell models [19] at 660 nm [20]. Studies have also shown that it enhances diabetic wound healing in both rats and mice [21–23]. Photobiostimulation in the visible and NIR spectral range has been demonstrated to regulate gene expression in human and animal cell cultures, even though its effect was not consistent in all irradiated cells [24]. Studies from different areas showed variations in the gene expression profile of 50 cultures of fibroblasts [25]. Few studies have exploited the relationship of laser irradiation and gene expression of the ECM in fibroblasts *in vitro*. Due to previous studies which showed an increase in collagen type I (Col-I) in response to laser irradiation at 660 nm [20], this study aimed to determine the effect of laser irradiation at 660 nm on the gene expression profile of the ECM and its cell adhesion molecules.

2. Methodology

2.1. Cell Culture. This study was performed on human skin fibroblasts isolated from a consenting adult undergoing abdominoplasty (Linksfeld, Sandringham, Johannesburg) (University of Johannesburg Academic Ethics Committee Clearance Reference number 01/06). Cells were seeded into 3.4 cm diameter tissue culture flasks at a density of 6×10^5 and routinely cultured according to standard techniques [26]. Different cell models, namely, normal (N), normal wounded (NW), and diabetic wounded (DW), were used. To establish an *in vitro* diabetic model, 17 mM/L D-glucose was added to the media with a base concentration of 5.6 mM/L D-glucose. Thirty minutes prior to irradiation, a sterile 1 mL disposable pipette was used to scratch the monolayer of cells in a streaking motion (i.e., creating a central scratch (CS)). This creates a cell-free zone on either side of the central scratch [27, 28].

2.2. Laser Irradiation. Cells were irradiated with 5 J/cm² using a continuous wave diode laser emitting at a wavelength

TABLE 3: Gene expression profile in normal (N) cells irradiated at 660 nm. Total RNA from nonirradiated N cells and irradiated N cells were characterised in triplicate. A fold difference >1 is considered as gene upregulation, while a fold difference <1 is considered as gene downregulation. Fold differences are indicated as upregulation (\uparrow) or downregulation (\downarrow). X denotes the nonsignificant genes in that particular cell model.

Gene symbol	Gene description	Gene ID	Fold difference	Up/downregulation	<i>P</i> value
ADAMTS1	ADAM metalloproteinase with thrombospondin type 1 motif, 1	9510	4.36	\uparrow	0.003
ADAMTS13	ADAM metalloproteinase with thrombospondin type 1 motif, 13	11093	1.32	X	0.259
ADAMTS8	ADAM metalloproteinase with thrombospondin type 1 motif, 8	11095	2.77	\uparrow	0.003
CD44	CD44 molecule (Indian blood group)	960	4.85	\uparrow	0.012
CDH1	Cadherin 1, type 1, E-cadherin (epithelial)	999	0.58	\downarrow	0.019
CLEC3B	C-type lectin domain family 3, member B	7123	1.90	X	0.078
CNTN1	Contactin 1	1272	1.14	X	0.547
COL11A1	Collagen, type XI, alpha 1	1301	1.05	X	0.896
COL12A1	Collagen, type XII, alpha 1	1303	2.21	\uparrow	0.003
COL14A1	Collagen, type XIV, alpha 1	7373	0.56	X	0.116
COL15A1	Collagen, type XV, alpha 1	1306	1.33	X	0.198
COL16A1	Collagen, type XVI, alpha 1	1307	1.57	X	0.074
COL1A1	Collagen, type I, alpha 1	1277	1.88	\uparrow	0.001
COL4A2	Collagen, type IV, alpha 2	1284	1.78	\uparrow	0.022
COL5A1	Collagen, type V, alpha 1	1289	4.23	\uparrow	0.001
COL6A1	Collagen, type VI, alpha 1	1291	2.42	\uparrow	0.010
COL6A2	Collagen, type VI, alpha 2	1292	3.99	\uparrow	0.000
COL7A1	Collagen, type VII, alpha 1	1294	1.13	X	0.658
COL8A1	Collagen, type VIII, alpha 1	1295	3.07	\uparrow	0.000
CTGF	Connective tissue growth factor	1490	0.43	\downarrow	0.002
CTNNA1	Catenin (cadherin-associated protein), alpha 1, 102 kDa	1495	0.73	\downarrow	0.039
CTNNB1	Catenin (cadherin-associated protein), beta 1, 88 kDa	1499	1.27	X	0.153
CTNND1	Catenin (cadherin-associated protein), delta 1	1500	2.21	\uparrow	0.001
CTNND2	Catenin (cadherin-associated protein), delta 2 (neural plakophilin-related arm-repeat protein)	1501	0.09	\downarrow	0.002
ECM1	Extracellular matrix protein 1	1893	0.47	\downarrow	0.000
FN1	Fibronectin 1	2335	2.29	\uparrow	0.005
HAS1	Hyaluronan synthase 1	3036	1.20	X	0.182
ICAM1	Intercellular adhesion molecule 1	3383	0.72	X	0.156
ITGA1	Integrin, alpha 1	3672	1.88	\uparrow	0.002
ITGA2	Integrin, alpha 2 (CD49B, alpha 2 subunit of VLA-2 receptor)	3673	0.99	X	0.650
ITGA3	Integrin, alpha 3 (antigen CD49C, alpha 3 subunit of VLA-3 receptor)	3675	2.98	\uparrow	0.000
ITGA4	Integrin, alpha 4 (antigen CD49D, alpha 4 subunit of VLA-4 receptor)	3676	0.81	X	0.193
ITGA5	Integrin, alpha 5 (fibronectin receptor, alpha polypeptide)	3678	3.26	\uparrow	0.000
ITGA6	Integrin, alpha 6	3655	1.21	X	0.085
ITGA7	Integrin, alpha 7	3679	0.92	X	0.780
ITGA8	Integrin, alpha 8	8516	1.06	X	0.805

TABLE 3: Continued.

Gene symbol	Gene description	Gene ID	Fold difference	Up/downregulation	P value
ITGAL	Integrin, alpha L (antigen CD11A (p180), lymphocyte function-associated antigen 1; alpha polypeptide)	3683	1.06	X	0.540
ITGAM	Integrin, alpha M (complement component 3 receptor 3 subunit)	3684	1.58	X	0.055
ITGAV	Integrin, alpha V (vitronectin receptor, alpha polypeptide, antigen CD51)	3685	1.17	X	0.331
ITGB1	Integrin, beta 1 (fibronectin receptor, beta polypeptide, antigen CD29 includes MDF2, MSK12)	3688	0.92	X	0.459
ITGB2	Integrin, beta 2 (complement component 3 receptor 3 and 4 subunit)	3689	0.96	X	0.792
ITGB3	Integrin, beta 3 (platelet glycoprotein IIIa, antigen CD61)	3690	1.08	X	0.339
ITGB4	Integrin, beta 4	3691	1.25	X	0.127
ITGB5	Integrin, beta 5	3693	1.05	X	0.672
KAL1	Kallmann syndrome 1 sequence	3730	1.53	↑	0.030
LAMA1	Laminin, alpha 1	284217	0.52	↓	0.001
LAMA2	Laminin, alpha 2	3908	0.52	↓	0.008
LAMA3	Laminin, alpha 33909	3909	2.60	↑	0.023
LAMB1	Laminin, beta 1	3912	0.92	X	0.594
LAMB3	Laminin, beta 3	3914	0.55	X	0.069
LAMC1	Laminin, gamma 1 (formerly LAMB2)	3915	0.83	X	0.063
MMP1	Matrix metalloproteinase 1 (interstitial collagenase)	4312	0.41	↓	0.001
MMP10	Matrix metalloproteinase 10 (stromelysin 2)	4319	0.81	X	0.198
MMP11	Matrix metalloproteinase 11 (stromelysin 3)	4320	1.53	↑	0.015
MMP12	Matrix metalloproteinase 12 (macrophage elastase)	4321	0.48	↓	0.010
MMP13	Matrix metalloproteinase 13 (collagenase 3)	4322	0.42	↓	0.001
MMP14	Matrix metalloproteinase 14 (membrane-inserted)	4323	4.14	↑	0.000
MMP15	Matrix metalloproteinase 15 (membrane-inserted)	4324	1.96	↑	0.000
MMP16	Matrix metalloproteinase 16 (membrane-inserted)	4325	1.11	X	0.186
MMP2	Matrix metalloproteinase 2 (gelatinase A, 72 kDa gelatinase, 72 kDa type IV collagenase)	4313	3.34	↑	0.000
MMP3	Matrix metalloproteinase 3 (stromelysin 1, progelatinase)	4314	0.23	↓	0.007
MMP7	Matrix metalloproteinase 7 (matrilysin, uterine)	4316	0.62	↓	0.045
MMP8	Matrix metalloproteinase 8 (neutrophil collagenase)	4317	0.75	X	0.112
MMP9	Matrix metalloproteinase 9 (gelatinase B, 92 kDa gelatinase, 92 kDa type IV collagenase)	4318	0.39	↓	0.013
NCAM1	Neural cell adhesion molecule 1	4684	1.63	↑	0.027
PECAM1	Platelet/endothelial cell adhesion molecule	5175	0.81	X	0.503
SELE	Selectin E	6401	0.93	X	0.568
SELL	Selectin L	6402	0.99	X	0.961
SELP	Selectin P (granule membrane protein 140 kDa, antigen CD62)	6403	1.35	X	0.469
SGCE	Sarcoglycan, epsilon	8910	0.36	↓	0.004
SPARC	Secreted protein, acidic, cysteine-rich (osteonectin)	6678	3.33	↑	0.000

TABLE 3: Continued.

Gene symbol	Gene description	Gene ID	Fold difference	Up/downregulation	P value
SPG7	Spastic paraplegia 7 (pure and complicated autosomal recessive)	6687	5.12	↑	0.000
SPP1	Secreted phosphoprotein 1	6696	0.55	↓	0.001
TGFBI	Transforming growth factor, beta-induced, 68 kDa	7045	0.87	X	0.361
THBS1	Thrombospondin 1	7057	1.87	↑	0.006
THBS2	Thrombospondin 2	7058	2.65	↑	0.003
THBS3	Thrombospondin 3	7059	1.20	X	0.235
TIMP1	TIMP metalloproteinase inhibitor 1	7076	1.43	↑	0.035
TIMP2	TIMP metalloproteinase inhibitor 2	7077	1.17	↑	0.025
TIMP3	TIMP metalloproteinase inhibitor 3	7078	0.43	↓	0.008
TNC	Tenascin C	3371	0.49	↓	0.002
VCAMI	Vascular cell adhesion molecule 1	7412	0.38	↓	0.010
VCAN	Versican	1462	0.46	↓	0.008
VTN	Vitronectin	7448	1.12	X	0.585

of 660 nm (Fremont, CA, USA, RGLase, TECIRL-100G-650SMA); laser parameters are shown in Table 1. All lasers were supplied and set up by the National Laser Centre (NLC) of the Council for Scientific and Industrial Research (CSIR), South Africa. Nonirradiated (0 J/cm^2) normal cells (for irradiated normal and normal wounded) and diabetic wounded cells (for irradiated diabetic wounded cells) served as the control groups. Cells were irradiated from above, with the culture dish lid off, in 1 mL culture media and in the dark to omit nuisance variables suggestive of polychromatic light that would interfere with the laser effect. The power output was measured using a power meter (FieldMate, 0398D05) at bench level prior to each irradiation, and the readings were used to determine the irradiation time. The temperature of the culture media during irradiation was measured every 2 min and remained less than 32°C . Cells were incubated for 48 h, and the profile of genes involved in the ECM and cell adhesion molecules were assessed using a real-time reverse transcription quantitative polymerase chain reaction (RT-qPCR) array.

2.3. RNA Isolation and Purity. Isolation of total RNA from the cells was performed on the Qiagen QIAcube (Whitehead Scientific, Cape Town, South Africa) using the RNeasy Mini Kit (Whitehead Scientific, Cape Town, South Africa, Qiagen, 74104) including QIAshredder homogenizers (Whitehead Scientific, Cape Town, South Africa, Qiagen, 79654). After incubation, cell cultures were detached with TrypLE Express ($1 \text{ mL}/25 \text{ cm}^2$) (Life Technologies, Gibco, Invitrogen, 12605-021) and washed with phosphate buffered saline (PBS) to eliminate traces of culture media and then resuspended in $600 \mu\text{L}$ of a guanidine-thiocyanate-containing buffer (RLT buffer) to disrupt the cells, inactivate RNases, and release cellular contents. Within 30 min, $30 \mu\text{L}$ of total RNA was eluted and quantified. The concentration of RNA was established using the Quant-iT RNA Assay Kits (Life Technologies, Johannesburg, South Africa, Invitrogen, Q32852) with the Invitrogen Qubit 2.0 fluorometer (Life Technologies,

Johannesburg, South Africa). The ratio between absorbance 260 and 280 nm ($A_{260 \text{ nm}}/A_{280 \text{ nm}}$) was used to estimate the sample purity using a UV/Vis spectrophotometer (Separation Scientific, Johannesburg, South Africa, PerkinElmer, Victor³).

2.4. cDNA Synthesis. According to the protocol, a two-step procedure was used to synthesise cDNA using the QuantiTect Reverse Transcription Kit (Whitehead Scientific, Cape Town, South Africa, Qiagen, 205311). Traces of possible contaminating genomic DNA (gDNA) was eliminated from $1 \mu\text{g}$ purified RNA sample using the gDNA Wipeout Buffer for 2 min at 42°C . RNA was then reverse-transcribed using a reverse transcription (RT) master mix. Six microliters of RT master mix was added to the reaction mixture to give a final volume of $20 \mu\text{L}$. The mixture was then incubated for 30 min at 42°C and thereafter 3 min at 95°C to terminate the reaction. One microliter of sample was used to estimate the purity as stated earlier. Samples were stored on ice to proceed directly with real-time qPCR or stored at -20°C .

2.5. Gene Expression Profiling. Real-time qPCR was performed using the SABiosciences RT² profiler PCR array (Whitehead Scientific, Cape Town, South Africa, PAHS-01321Z) which profiled 84 genes (Table 2). Ninety-two microliters of PCR water (Diethyl Pyrocarbonate, DEPC free) was added to thawed cDNA ($19 \mu\text{L}$) giving a final volume of $111 \mu\text{L}$. One hundred and two microliters of diluted cDNA was added to the ready-to-use 2x SABiosciences RT² qPCR master mix (330521), and then $1248 \mu\text{L}$ of PCR water was added to give a total volume of $2700 \mu\text{L}$. Components were mixed and $25 \mu\text{L}$ of the experimental cocktail was dispensed into each well of the 96-well plate. The sealed PCR plates were centrifuged at 1000 g (Separation Scientific, Johannesburg, South Africa, Thermo Scientific, Heraeus Labofuge 400) for 1 min to remove any bubbles and run in the preset real-time thermocycler (Anatech, Randburg, South Africa, Stratagene

TABLE 4: Gene expression profile in normal wounded (NW) cells irradiated at 660 nm. Total RNA from nonirradiated N cells and irradiated NW cells were characterised in triplicate. A fold difference >1 is considered as gene upregulation, while a fold difference <1 is considered as gene downregulation. Fold differences are indicated as upregulation (↑) or downregulation (↓). X denotes the nonsignificant genes in that particular cell model.

Gene symbol	Gene description	Gene ID	Fold difference	Up/downregulation	P value
ADAMTS1	ADAM metalloproteinase with thrombospondin type 1 motif, 1	9510	1.86	↑	0.045
ADAMTS13	ADAM metalloproteinase with thrombospondin type 1 motif, 13	11093	2.39	↑	0.003
ADAMTS8	ADAM metalloproteinase with thrombospondin type 1 motif, 8	11095	1.85	↑	0.001
CD44	CD44 molecule (Indian blood group)	960	1.25	X	0.356
CDH1	Cadherin 1, type 1, E-cadherin (epithelial)	999	1.23	X	0.205
CLEC3B	C-type lectin domain family 3, member B	7123	1.15	X	0.299
CNTN1	Contactin 1	1272	1.25	X	0.068
COL1A1	Collagen, type XI, alpha 1	1301	1.04	X	0.854
COL12A1	Collagen, type XII, alpha 1	1303	1.69	↑	0.004
COL14A1	Collagen, type XIV, alpha 1	7373	0.81	X	0.370
COL15A1	Collagen, type XV, alpha 1	1306	1.20	X	0.216
COL16A1	Collagen, type XVI, alpha 1	1307	1.05	X	0.749
COL1A1	Collagen, type I, alpha 1	1277	1.45	↑	0.006
COL4A2	Collagen, type IV, alpha 2	1284	1.44	X	0.069
COL5A1	Collagen, type V, alpha 1	1289	1.61	↑	0.005
COL6A1	Collagen, type VI, alpha 1	1291	1.27	X	0.170
COL6A2	Collagen, type VI, alpha 2	1292	1.36	X	0.105
COL7A1	Collagen, type VII, alpha 1	1294	1.42	↑	0.005
COL8A1	Collagen, type VIII, alpha 1	1295	1.36	↑	0.011
CTGF	Connective tissue growth factor	1490	0.95	X	0.284
CTNNA1	Catenin (cadherin-associated protein), alpha 1, 102 kDa	1495	1.03	X	0.720
CTNNA1	Catenin (cadherin-associated protein), beta 1, 88 kDa	1499	0.95	X	0.700
CTNNA1	Catenin (cadherin-associated protein), delta 1	1500	1.36	X	0.105
CTNNA2	Catenin (cadherin-associated protein), delta 2 (neural plakophilin-related arm-repeat protein)	1501	0.63	↓	0.019
ECM1	Extracellular matrix protein 1	1893	0.75	↓	0.017
FN1	Fibronectin 1	2335	1.63	↑	0.012
HAS1	Hyaluronan synthase 1	3036	2.00	↑	0.005
ICAM1	Intercellular adhesion molecule 1	3383	0.78	X	0.139
ITGA1	Integrin, alpha 1	3672	1.57	↑	0.005
ITGA2	Integrin, alpha 2 (CD49B, alpha 2 subunit of VLA-2 receptor)	3673	0.86	X	0.073
ITGA3	Integrin, alpha 3 (antigen CD49C, alpha 3 subunit of VLA-3 receptor)	3675	1.33	X	0.121
ITGA4	Integrin, alpha 4 (antigen CD49D, alpha 4 subunit of VLA-4 receptor)	3676	1.19	X	0.057
ITGA5	Integrin, alpha 5 (fibronectin receptor, alpha polypeptide)	3678	1.46	↑	0.021
ITGA6	Integrin, alpha 6	3655	1.55	↑	0.016
ITGA7	Integrin, alpha 7	3679	0.90	X	0.462
ITGA8	Integrin, alpha 8	8516	2.94	↑	0.012
ITGAL	Integrin, alpha L (antigen CD11A (p180), lymphocyte function-associated antigen 1; alpha polypeptide) 3683	3683	2.04	↑	0.030
ITGAM	Integrin, alpha M (complement component 3 receptor 3 subunit) 3684	3684	1.59	↑	0.027

TABLE 4: Continued.

Gene symbol	Gene description	Gene ID	Fold difference	Up/downregulation	P value
ITGAV	Integrin, alpha V (vitronectin receptor, alpha polypeptide, antigen CD51)	3685	1.43	↑	0.013
ITGB1	Integrin, beta 1 (fibronectin receptor, beta polypeptide, antigen CD29 includes MDF2, MSK12)	3688	1.05	X	0.652
ITGB2	Integrin, beta 2 (complement component 3 receptor 3 and 4 subunit)	3689	1.17	X	0.259
ITGB3	Integrin, beta 3 (platelet glycoprotein IIIa, antigen CD61)	3690	1.53	↑	0.007
ITGB4	Integrin, beta 4	3691	1.42	X	0.062
ITGB5	Integrin, beta 5	3693	1.07	X	0.539
KAL1	Kallmann syndrome 1 sequence	3730	1.41	↑	0.006
LAMA1	Laminin, alpha 1	284217	0.81	X	0.096
LAMA2	Laminin, alpha 2	3908	1.01	X	0.921
LAMA3	Laminin, alpha 33909	3909	1.33	X	0.546
LAMB1	Laminin, beta 1	3912	1.18	X	0.113
LAMB3	Laminin, beta 3	3914	0.87	X	0.273
LAMC1	Laminin, gamma 1 (formerly LAMB2)	3915	0.94	X	0.419
MMP1	Matrix metalloproteinase 1 (interstitial collagenase)	4312	0.53	↓	0.011
MMP10	Matrix metalloproteinase 10 (stromelysin 2)	4319	1.06	X	0.456
MMP11	Matrix metalloproteinase 11 (stromelysin 3)	4320	1.60	↑	0.009
MMP12	Matrix metalloproteinase 12 (macrophage elastase)	4321	0.75	X	0.019
MMP13	Matrix metalloproteinase 13 (collagenase 3)	4322	0.78	X	0.075
MMP14	Matrix metalloproteinase 14 (membrane-inserted)	4323	0.97	X	0.909
MMP15	Matrix metalloproteinase 15 (membrane-inserted)	4324	2.66	↑	0.000
MMP16	Matrix metalloproteinase 16 (membrane-inserted)	4325	1.00	X	0.963
MMP2	Matrix metalloproteinase 2 (gelatinase A, 72 kDa gelatinase, 72 kDa type IV collagenase)	4313	1.52	↑	0.004
MMP3	Matrix metalloproteinase 3 (stromelysin 1, progelatinase)	4314	0.33	↓	0.005
MMP7	Matrix metalloproteinase 7 (matrilysin, uterine)	4316	1.15	X	0.499
MMP8	Matrix metalloproteinase 8 (neutrophil collagenase)	4317	1.53	↑	0.049
MMP9	Matrix metalloproteinase 9 (gelatinase B, 92 kDa gelatinase, 92 kDa type IV collagenase)	4318	1.02	X	0.803
NCAM1	Neural cell adhesion molecule 1	4684	1.09	X	0.475
PECAM1	Platelet/endothelial cell adhesion molecule	5175	2.24	↑	0.009
SELE	Selectin E	6401	1.39	↑	0.041
SELL	Selectin L	6402	1.08	X	0.597
SELP	Selectin P (granule membrane protein 140 kDa, antigen CD62)	6403	1.47	↑	0.032
SGCE	Sarcoglycan, epsilon	8910	0.73	↓	0.034
SPARC	Secreted protein, acidic, cysteine-rich (osteonectin)	6678	1.59	↑	0.001
SPG7	Spastic paraplegia 7 (pure and complicated autosomal recessive)	6687	1.28	↑	0.042
SPP1	Secreted phosphoprotein 1	6696	0.84	X	0.118
TGFBI	Transforming growth factor, beta-induced, 68 kDa	7045	1.10	X	0.317
THBS1	Thrombospondin 1	7057	1.59	↑	0.008
THBS2	Thrombospondin 2	7058	2.04	↑	0.004
THBS3	Thrombospondin 3	7059	0.89	X	0.349
TIMP1	TIMP metalloproteinase inhibitor 1	7076	1.31	X	0.073
TIMP2	TIMP metalloproteinase inhibitor 2	7077	1.07	X	0.244
TIMP3	TIMP metalloproteinase inhibitor 3	7078	0.89	X	0.340

TABLE 4: Continued.

Gene symbol	Gene description	Gene ID	Fold difference	Up/downregulation	<i>P</i> value
TNC	Tenascin C	3371	0.73	↓	0.005
VCAM1	Vascular cell adhesion molecule 1	7412	0.61	X	0.065
VCAN	Versican	1462	0.87	X	0.252
VTN	Vitronectin	7448	0.62	↓	0.024

Mx3000p). The thermocycler profile setting was 10 min at 95°C for 1 cycle and 15 s at 95°C and 1 min at 60°C for 40 cycles. The software was also programmed to do a melt or dissociation curve at the end of the run to ensure the amplification of a single product for each gene. The threshold cycle (C_t) values were imported into an Excel spreadsheet (Available from the SABiosciences website: <http://www.sabiosciences.com/>) which normalised the results against the 5 housekeeping genes (ACTB, B2M, GAPDH, HPRTI, and RPLPO). In addition, the relative gene expression ($\Delta\Delta C_t$) and fold change ($2^{-\Delta\Delta C_t}$) were also calculated. Prior to data analysis, all the C_t values of the controls were examined to ensure proper functioning of the PCR array and preceding steps (positive PCR control, C_t value of 20 ± 2 ; genomic DNA control, C_t value of >35). A fold change of >1 was reported as fold upregulation and a fold change <1 was reported as fold downregulation.

2.6. Statistical Analysis. Experiments were repeated three times ($n = 3$). Student's *t*-test was analysed based on the replicate fold change for each gene in both the test and the control groups by the SABiosciences Excel-based data analysis template and reported as significant if $P < 0.05$. Results are represented in Tables 3 to 6.

3. Results

Irradiation of N cells with 660 nm resulted in the significant upregulation of 29 genes and downregulation of 19 genes (Table 3). Irradiation of NW cells with 660 nm resulted in the significant upregulation of 32 genes and downregulation of 6 genes (Table 4). Irradiation of DW cells with 660 nm resulted in the upregulation of 18 genes and downregulation of 31 genes (Table 5). A summary of the results is presented in Table 6.

4. Discussion and Conclusion

ECM components are very useful in different aspects of wound healing. The ECM interacts with various cells and growth factors in cell proliferation, influencing migration, cell differentiation, and regulating several biological responses [1, 5, 6, 29, 30]. The effects shown by different ECM components depend on the stage of the wound and are determined by the interactions between the cells and growth factors [29]. There is great need for gene expression profiling in the ECM following laser irradiation to be exploited. In this study, 84 genes related to the ECM were studied in

various models. Photoirradiation was shown to stimulate gene expression 48 h after incubation in irradiated N, NW, and DW cells as compared to their respective controls. The genes, either up- or downregulated, are functionally grouped depending on their pathways in the ECM.

In the present study, four main CAM families were mediated following irradiation at 660 nm. They include cadherins, integrins, selectins, and immunoglobulin CAM (Ig-CAM). The cadherin family are mainly calcium-dependent glycoproteins containing an extracellular domain, a transmembrane domain, and an intracellular domain [31]. Cadherins and integrins form the main cell-surface transmembrane receptors and are involved in modulating cell-cell and cell-matrix adhesion. They function in various cellular events, namely, cell migration, proliferation, survival, differentiation, and modulation of gene expression profiling [32, 33]. In irradiated N cells, CTNND2 was upregulated and CDH1, CTNNA1, and CTNND1 were downregulated at 660 nm; irradiated NW cells showed downregulation of CTNND2; and DW cells showed an upregulation of CDH1 and CTNND2, while CTNND1 was downregulated.

Integrins are the main receptor family in charge of interactions in the ECM and consist of two noncovalent α and β subunits; the specific combination of the subunits determines the degree of cell signalling [34]. In irradiated N cells, ITGA1, ITGA3, ITGA5, and ITGAM were upregulated; in irradiated NW cells, ITGA1, ITGA5, ITGA6, ITGA8, ITGAL, ITGAM, ITGAV, and ITGB3 were upregulated; and in irradiated DW cells, ITGA8, ITGAL, and ITGB3 were upregulated, while ITGA2, ITGA3, ITGA5, ITGA6, ITGB1, and ITGB4 were downregulated.

Selectins consist of an extracellular domain with a calcium-dependent lectin domain, an epidermal growth factor domain, and a hydrophobic transmembrane domain [35, 36]. Selectins expressed in response to laser irradiation in N cells included CLEC3B, while NW cells showed an upregulation in SELE, SELL, and SELP and in DW cells there was an upregulation in SELL.

Ig-CAM contains an extracellular domain with FN repeats, a transmembrane domain, and an intracellular domain [31, 35]. These domains bind with proteins of the ECM, namely, collagen, LMN, and FN, as well as certain integral cell-surface proteins [31]. Members of the Ig-CAM family expressed in response to LILI were CD44, FN1, NCAM1, PECAM1, SGCE, THBS1, THBS2, SPP1, VTN, VCAM1, and CNTN1. In irradiated N cells, CD44, FN1, NCAM1, THBS1, and THBS2 were upregulated, while SGCE, VCAM1, and SPP1 were downregulated following irradiation at 660 nm as compared to nonirradiated N cells. In irradiated NW cells,

TABLE 5: Gene expression profile in diabetic wounded (DW) cells irradiated at 660 nm. Total RNA from nonirradiated DW cells and irradiated DW cells were characterised in triplicate. A fold difference >1 is considered as gene upregulation, while a fold difference <1 is considered as gene downregulation. Fold differences are indicated as upregulation (↑) or downregulation (↓). X denotes the nonsignificant genes in that particular cell model.

Gene symbol	Gene description	Gene ID	Fold difference	Up/downregulation	<i>P</i> value
ADAMTS1	ADAM metalloproteinase with thrombospondin type 1 motif, 1	9510	0.50	↓	0.003
ADAMTS13	ADAM metalloproteinase with thrombospondin type 1 motif, 13	11093	0.91	X	0.589
ADAMTS8	ADAM metalloproteinase with thrombospondin type 1 motif, 8	11095	2.75	↑	0.005
CD44	CD44 molecule (Indian blood group)	960	0.53	↓	0.049
CDH1	Cadherin 1, type 1, E-cadherin (epithelial)	999	2.12	↑	0.051
CLEC3B	C-type lectin domain family 3, member B	7123	1.14	X	0.749
CNTN1	Contactin 1	1272	2.19	↑	0.041
COL1A1	Collagen, type XI, alpha 1	1301	3.68	↑	0.002
COL12A1	Collagen, type XII, alpha 1	1303	0.37	X	0.003
COL14A1	Collagen, type XIV, alpha 1	7373	1.24	↑	0.023
COL15A1	Collagen, type XV, alpha 1	1306	0.67	X	0.082
COL16A1	Collagen, type XVI, alpha 1	1307	0.61	↓	0.001
COL1A1	Collagen, type I, alpha 1	1277	0.87	X	0.498
COL4A2	Collagen, type IV, alpha 2	1284	0.99	X	0.966
COL5A1	Collagen, type V, alpha 1	1289	0.56	↓	0.036
COL6A1	Collagen, type VI, alpha 1	1291	0.64	↓	0.015
COL6A2	Collagen, type VI, alpha 2	1292	0.58	↓	0.014
COL7A1	Collagen, type VII, alpha 1	1294	0.36	↓	0.017
COL8A1	Collagen, type VIII, alpha 1	1295	0.71	X	0.271
CTGF	Connective tissue growth factor	1490	1.10	X	0.521
CTNNA1	Catenin (cadherin-associated protein), alpha 1, 102 kDa	1495	0.83	X	0.340
CTNNA1	Catenin (cadherin-associated protein), beta 1, 88 kDa	1499	0.64	X	0.084
CTNND1	Catenin (cadherin-associated protein), delta 1	1500	0.36	↓	0.005
CTNND2	Catenin (cadherin-associated protein), delta 2 (neural plakophilin-related arm-repeat protein)	1501	2.72	↑	0.052
ECM1	Extracellular matrix protein 1	1893	0.74	X	0.076
FN1	Fibronectin 1	2335	0.58	↓	0.008
HAS1	Hyaluronan synthase 1	3036	0.87	X	0.544
ICAM1	Intercellular adhesion molecule 1	3383	0.97	X	0.843
ITGA1	Integrin, alpha 1	3672	0.97	X	0.721
ITGA2	Integrin, alpha 2 (CD49B, alpha 2 subunit of VLA-2 receptor)	3673	0.52	↓	0.015
ITGA3	Integrin, alpha 3 (antigen CD49C, alpha 3 subunit of VLA-3 receptor)	3675	0.50	↓	0.010
ITGA4	Integrin, alpha 4 (antigen CD49D, alpha 4 subunit of VLA-4 receptor)	3676	0.86	X	0.459
ITGA5	Integrin, alpha 5 (fibronectin receptor, alpha polypeptide)	3678	0.54	↓	0.004
ITGA6	Integrin, alpha 6	3655	0.76	↓	0.012
ITGA7	Integrin, alpha 7	3679	1.11	X	0.513
ITGA8	Integrin, alpha 8	8516	2.75	↑	0.051
ITGAL	Integrin, alpha L (antigen CD11A (p180), lymphocyte function-associated antigen 1; alpha polypeptide) 3683	3683	1.89	↑	0.003
ITGAM	Integrin, alpha M (complement component 3 receptor 3 subunit)	3684	1.77	X	0.065

TABLE 5: Continued.

Gene symbol	Gene description	Gene ID	Fold difference	Up/downregulation	P value
ITGAV	Integrin, alpha V (vitronectin receptor, alpha polypeptide, antigen CD51)	3685	0.50	↓	0.002
ITGB1	Integrin, beta 1 (fibronectin receptor, beta polypeptide, antigen CD29 includes MDF2, MSK12)	3688	0.53	↓	0.005
ITGB2	Integrin, beta 2 (complement component 3 receptor 3 and 4 subunit)	3689	1.58	X	0.083
ITGB3	Integrin, beta 3 (platelet glycoprotein IIIa, antigen CD61)	3690	0.58	↓	0.006
ITGB4	Integrin, beta 4	3691	1.87	↑	0.041
ITGB5	Integrin, beta 5	3693	0.97	X	0.879
KAL1	Kallmann syndrome 1 sequence	3730	0.41	↓	0.001
LAMA1	Laminin, alpha 1	284217	0.60	↓	0.014
LAMA2	Laminin, alpha 2	3908	1.17	X	0.396
LAMA3	Laminin, alpha 3	3909	2.25	↑	0.031
LAMB1	Laminin, beta 1	3912	0.95	X	0.609
LAMB3	Laminin, beta 3	3914	0.61	↓	0.010
LAMC1	Laminin, gamma 1 (formerly LAMB2)	3915	0.54	↓	0.008
MMP1	Matrix metalloproteinase 1 (interstitial collagenase)	4312	0.38	↓	0.001
MMP10	Matrix metalloproteinase 10 (stromelysin 2)	4319	1.28	X	0.271
MMP11	Matrix metalloproteinase 11 (stromelysin 3)	4320	1.71	↑	0.025
MMP12	Matrix metalloproteinase 12 (macrophage elastase)	4321	0.52	↓	0.005
MMP13	Matrix metalloproteinase 13 (collagenase 3)	4322	1.89	↑	0.034
MMP14	Matrix metalloproteinase 14 (membrane-inserted)	4323	0.44	↓	0.016
MMP15	Matrix metalloproteinase 15 (membrane-inserted)	4324	1.24	X	0.157
MMP16	Matrix metalloproteinase 16 (membrane-inserted)	4325	0.44	↓	0.003
MMP2	Matrix metalloproteinase 2 (gelatinase A, 72 kDa gelatinase, 72 kDa type IV collagenase)	4313	0.54	↓	0.002
MMP3	Matrix metalloproteinase 3 (stromelysin 1, progelatinase)	4314	2.42	↑	0.009
MMP7	Matrix metalloproteinase 7 (matrilysin, uterine)	4316	1.86	↑	0.024
MMP8	Matrix metalloproteinase 8 (neutrophil collagenase)	4317	0.63	↓	0.029
MMP9	Matrix metalloproteinase 9 (gelatinase B, 92 kDa gelatinase, 92 kDa type IV collagenase)	4318	1.47	↑	0.009
NCAM1	Neural cell adhesion molecule 1	4684	0.97	X	0.811
PECAM1	Platelet/endothelial cell adhesion molecule	5175	3.66	X	0.213
SELE	Selectin E	6401	1.50	X	0.078
SELL	Selectin L	6402	2.36	↑	0.013
SELP	Selectin P (granule membrane protein 140 kDa, antigen CD62)	6403	1.90	X	0.249
SGCE	Sarcoglycan, epsilon	8910	0.93	X	0.657
SPARC	Secreted protein, acidic, cysteine-rich (osteonectin)	6678	0.66	↓	0.054
SPG7	Spastic paraplegia 7 (pure and complicated autosomal recessive)	6687	0.48	↓	0.005
SPP1	Secreted phosphoprotein 1	6696	0.58	↓	0.009
TGFB1	Transforming growth factor, beta-induced, 68 kDa	7045	0.79	X	0.099
THBS1	Thrombospondin 1	7057	0.35	↓	0.001
THBS2	Thrombospondin 2	7058	0.81	X	0.088
THBS3	Thrombospondin 3	7059	1.03	X	0.794
TIMP1	TIMP metalloproteinase inhibitor 1	7076	1.47	↑	0.046

TABLE 5: Continued.

Gene symbol	Gene description	Gene ID	Fold difference	Up/downregulation	P value
TIMP2	TIMP metalloproteinase inhibitor 2	7077	0.93	X	0.788
TIMP3	TIMP metalloproteinase inhibitor 3	7078	1.05	X	0.825
TNC	Tenascin C	3371	1.18	X	0.492
VCAM1	Vascular cell adhesion molecule 1	7412	1.79	↑	0.002
VCAN	Versican	1462	0.96	X	0.775
VTN	Vitronectin	7448	1.20	X	0.240

FN1, PECAM1, THBS1, and THBS2 were upregulated, while SGCE and VTN were downregulated at 660 nm as compared to nonirradiated N cells. In irradiated DW cells, CNTN1 and VCAM1 were upregulated, while CD44, FN1, THBS1, and SPP1 were downregulated at 660 nm as compared to nonirradiated DW cells. Other adhesion molecules expressed in response to LILI were HAS1, VCAN, TNC, KALI, and CTGF. In this study, KALI was upregulated while TNC, VCAN, and CTGF were downregulated in irradiated N cells. In irradiated NW cells, HAS1 and KALI were upregulated and TNC was downregulated. In irradiated DW cells, KALI was upregulated at 660 nm as compared to nonirradiated DW cells.

ECM proteins including collagen, LMN, EI, proteoglycans, and FN have both adhesive and structural functions. The ECM maintains skin integrity and homeostasis and interacts with several structural and extracellular proteins. Collagen is encoded for by more than 42 genes [29, 37]. Some of the collagen molecules are formed through the interaction between FN and integrins [38, 39]. Collagens are extracellular proteins produced mainly by fibroblasts, divided into two main classes, namely, the nonfibril forming (collagens types IV, VI, VII, and XI) and the fibril forming collagens distinguished by their triple helix (collagens types I, II, III, V, and XI). Their main function is to maintain the structural integrity of various tissues and to strengthen and reorganise the ECM [40]. In this study, COL1A1, COL4A2, COL5A1, COL6A1, COL6A2, COL8A1, and COL12A1 were upregulated in irradiated N cells. In irradiated NW cells, COL1A1, COL5A1, COL7A1, COL8A1, and COL12A1 were upregulated, while in DW cells COL11A1 and COL14A1 were upregulated and COL5A1, COL6A1, COL6A2, COL7A1, COL12A1, and COL16A1 were downregulated.

LMNs are basement membrane proteins made up of three nonidentical chains. They are associated with cell adhesion, differentiation, migration, matrix organisation, and signal transduction. LAMA1 was upregulated in irradiated N cells, while LAMA2 and LAMA3 were downregulated. In irradiated DW cells LAMA3 was upregulated and LAMA1, LAMB3, and LAMC1 were downregulated. Other matrix associated proteins, such as secreted protein, acidic, and cysteine-rich (encoded for by SPARC), spastic paraplegin 7 (encoded for by SPG7), and extracellular matrix protein 1, were also evaluated. SPARC is associated with cell structure organisation, cell migration, and ECM synthesis [41, 42]. SPG7 is involved in the breakdown of incorrectly folded proteins intracellular motility, membrane trafficking, and organelle biogenesis [43].

ECM1 is part of a cluster of genes involved in epidermal differentiation. Irradiation of N and NW cells to 660 nm resulted in an upregulation of SPARC and SPG7 and a downregulation in ECM1. Analysis of the gene profile of irradiated DW cells revealed a significant downregulation of SPARC and SPG7. Significantly increased gene expression of the constituents of the basement membrane was observed at 660 nm in N and NW cells, while DW cells showed a decrease in gene regulation, with most of the genes downregulated.

MMPs are metalloproteinases involved in the degradation of the ECM and can be affected in normal or pathological tissue remodelling and wound healing with different substrates, mostly collagen. MMPs are inhibited by TIMPs. ADAMTS (a disintegrin and metalloproteinase with thrombospondin motifs) is a family of 19 peptidases that are involved in the processing of procollagen, connective tissue organization, and cell migration [44–48]. The gene profile for ECM proteases and inhibitors in response to irradiation at 660 nm revealed an upregulation in MMP2, MMP11, MMP14, MMP15, ADAMTS1, ADAMTS8, TIMP1, TIMP2, and TIMP3 and a downregulation in MMP1, MMP3, MMP7, MMP9, MMP12, and MMP13 in N cells. Irradiated NW cells showed an upregulation of MMP2, MMP8, MMP11, MMP15, ADAMTS1, ADAMTS8, and ADAMTS13, while MMP1, MMP3, and MMP12 showed a downregulation as compared to nonirradiated N cells. In irradiated DW cells, MMP3, MMP7, MMP9, MMP11, MMP13, ADAMTS8, and TIMP1 were upregulated, while ADAMTS1, MMP1, MMP2, MMP12, MMP14, and MMP16 were downregulated as compared to nonirradiated DW cells.

These results demonstrated changes in gene expression within the different irradiated N, NW, and DW cell models. The genetic profile seen in the N cell model is a normal response of fibroblast cells to laser irradiation at 660 nm with 5 J/cm². On the other hand, cells in the NW and DW models have been stressed and compromised in some way, and the genetic profile seen in these cells is a response of wounded/stressed fibroblast cells to laser irradiation at 660 nm. Mechanical modulation of these cells would increase upregulation of ECM components, ECM-specific receptors, and enhanced expression of several cytokines and growth factors in a time-dependent manner [49–51]. The present study showed that DW cells had a significantly downregulated gene expression profile as compared to N and NW cells when irradiated at 660 nm. The downregulation of most of the genes in DW cells is probably due to the dysfunctioning of the ECM exhibited in chronic wounds as a result of

TABLE 6: Summary of the various genes significantly expressed and their pathways in normal (N), normal wounded (NW), and diabetic wounded (DW) cells. Fold differences are indicated as upregulation (↑) or downregulation (↓). X denotes the nonsignificant genes in that particular cell model.

Gene symbol	Gene description	Gene pathway	N	NW	DW
ADAMTS1	ADAM metalloproteinase with thrombospondin type 1 motif, 1	ECM protease	↑	X	X
ADAMTS13	ADAM metalloproteinase with thrombospondin type 1 motif, 13	ECM protease, cell-matrix adhesion	X	↑	X
ADAMTS8	ADAM metalloproteinase with thrombospondin type 1 motif, 8	ECM protease	↑	↑	↑
CD44	CD44 molecule (Indian blood group)	Transmembrane, cell-cell adhesion	↑	X	↓
CDH1	Cadherin 1, type 1, E-cadherin (epithelial)	Transmembrane, cell-cell adhesion	↓	X	↓
CLEC3B	C-type lectin domain family 3, member B	Other adhesion and ECM molecules	↓	X	X
CNTN1	Contactin 1	Other adhesion molecules	X	X	↑
COL1A1	Collagen, type XI, alpha 1	Cell-cell adhesion, collagen, and ECM structure constituent	X	X	↑
COL12A1	Collagen, type XII, alpha 1	Other adhesion molecules, collagen, and ECM structure constituent	↑	↑	↓
COL14A1	Collagen, type XIV, alpha 1	Cell-cell adhesion, collagen, and ECM structure constituent	X	X	↑
COL16A1	Collagen, type XVI, alpha 1	Other adhesion molecules, collagen, and ECM structure constituent	X	X	↓
COL1A1	Collagen, type I, alpha 1	Collagen and ECM structure constituent	↑	↑	X
COL4A2	Collagen, type IV, alpha 2	Basement membrane constituent and ECM structure constituent	↑	X	X
COL5A1	Collagen, type V, alpha 1	Other adhesion molecules, collagen, and ECM structure constituent	↑	↑	↓
COL6A1	Collagen, type VI, alpha 1	Other adhesion molecules, collagen, and ECM structure constituent	↑	X	↓
COL6A2	Collagen, type VI, alpha 2	Cell-cell adhesion, collagen, and ECM structure constituent	↑	X	↓
COL7A1	Collagen, type VII, alpha 1	Other adhesion molecules, basement membrane constituent, collagen, ECM structure constituent, and ECM protease inhibitor	X	X	↓
COL8A1	Collagen, type VIII, alpha 1	Other adhesion molecules, collagen, and ECM structure constituent	↑	↑	X
CTGF	Connective tissue growth factor	Other adhesion and ECM molecules	↓	X	X
CTNNA1	Catenin (cadherin-associated protein), alpha 1, 102 kDa	Other adhesion molecules	↓	X	X
CTNND1	Catenin (cadherin-associated protein), delta 1	Cell-cell adhesion	↑	X	↓
CTNND2	Catenin (cadherin-associated protein), delta 2 (neural plakophilin-related arm-repeat protein)	Other adhesion molecules	↓	↓	↑

TABLE 6: Continued.

Gene symbol	Gene description	N	NW	DW
ECM1	Extracellular matrix protein 1	↓	↓	X
FN1	Fibronectin 1	↑	↑	↓
HAS1	Hyaluronan synthase 1	X	↑	X
ITGA1	Integrin, alpha 1	↑	↑	X
ITGA2	Integrin, alpha 2 (CD49B, alpha 2 subunit of VLA-2 receptor)	X	X	↓
ITGA3	Integrin, alpha 3 (antigen CD49C, alpha 3 subunit of VLA-3 receptor)	↑	X	↓
ITGA5	Integrin, alpha 5 (fibronectin receptor, alpha polypeptide)	↑	↑	↓
ITGA6	Integrin, alpha 6	X	↑	↓
ITGA8	Integrin, alpha 8	X	↑	↑
ITGAL	Integrin, alpha L (antigen CD11A (p180), lymphocyte function-associated antigen 1; alpha polypeptide)	X	↑	↑
ITGAM	Integrin, alpha M (complement component 3 receptor 3 subunit)	X	↑	X
ITGAV	Integrin, alpha V (vitronectin receptor, alpha polypeptide, antigen CD51)	X	↑	↓
ITGB1	Integrin, beta 1 (fibronectin receptor, beta polypeptide, antigen CD29 including MDF2, MSK12)	X	X	↓
ITGB3	Integrin, beta 3 (platelet glycoprotein IIIa, antigen CD61)	X	↑	↓
ITGB4	Integrin, beta 4	X	X	↑
KAL1	Kallmann syndrome 1 sequence	↑	↑	↓
LAMA1	Laminin, alpha 1	↓	X	X
LAMA2	Laminin, alpha 2	↓	X	X
LAMA3	Laminin, alpha 33909	↑	X	↑
LAMB3	Laminin, beta 3	X	X	↓
LAMC1	Laminin, gamma 1 (formerly LAMB2)	X	X	↓
MMP1	Matrix metalloproteinase 1 (interstitial collagenase)	↓	↓	↓
MMP11	Matrix metalloproteinase 11 (stromelysin 3)	↑	↑	↑
MMP12	Matrix metalloproteinase 12 (macrophage elastase)	↓	↓	↓
MMP13	Matrix metalloproteinase 13 (collagenase 3)	↓	X	↑
MMP14	Matrix metalloproteinase 14 (membrane-inserted)	↑	X	↓
MMP15	Matrix metalloproteinase 15 (membrane-inserted)	↑	↑	X

TABLE 6: Continued.

Gene symbol	Gene description	N	NW	DW
MMP16	Matrix metalloproteinase 16 (membrane-inserted)	X	X	↓
MMP2	Matrix metalloproteinase 2 (gelatinase A, 72 kDa gelatinase, and 72 kDa type IV collagenase)	↑	↑	↓
MMP3	Matrix metalloproteinase 3 (stromelysin 1 and progelatinase)	↓	↓	↑
MMP7	Matrix metalloproteinase 7 (matrilysin and uterine)	↓	X	↑
MMP8	Matrix metalloproteinase 8 (neutrophil collagenase)	X	↑	↓
MMP9	Matrix metalloproteinase 9 (gelatinase B, 92 kDa gelatinase, and 92 kDa type IV collagenase)	↓	X	↑
NCAM1	Neural cell adhesion molecule 1	↑	X	X
PECAM1	Platelet/endothelial cell adhesion molecule	X	↑	X
SELE	Selectin E	X	↑	X
SELL	Selectin L	X	X	↑
SELP	Selectin P (granule membrane protein 140 kDa and antigen CD62)	X	↑	X
SGCE	Sarcoglycan, epsilon	↓	↓	X
SPARC	Secreted protein, acidic, and cysteine-rich (osteonectin)	↑	↑	X
SPG7	Spastic paraplegia 7 (pure and complicated autosomal recessive)	↑	↑	↓
SPP1	Secreted phosphoprotein 1	↓	X	↓
THBS1	Thrombospondin 1	↑	↑	↓
THBS2	Thrombospondin 2	↑	↑	X
TIMPI	TIMP metalloproteinase inhibitor 1	↑	X	↑
TIMP2	TIMP metalloproteinase inhibitor 2	↑	X	X
TIMP3	TIMP metalloproteinase inhibitor 3	↓	X	X
TNC	Tenascin C	↓	↓	X
VCAM1	Vascular cell adhesion molecule 1	↓	X	↑
VCAN	Versican	↓	X	X
VTN	Vitronectin	X	↓	X

hyperglycaemia. Also in chronic wounds, the inflammatory phase is normally delayed, which promotes increased levels of proteases such as MMPs, causing destruction of the ECM, and damages growth factors as well as receptors essential in the healing process. This also results in a lack of integrins which bind to FN to enhance migration, and hence the decrease in migration [52, 53]. Furthermore MMP3, MMP7, MMP9, MMP11, and MMP13 were upregulated in DW cells irradiated at 660 nm. This is possibly due to the fact that degraded collagen molecules do not interact properly enabling a disorganised and weak ECM, increasing the levels of some MMPs in chronic wounds [54]. This corresponds with the decrease in Col-I seen in these cells [21]. However, there was a significant upregulation of some of the collagens and other essential ECM proteins, which is in line with the increase in collagen seen in irradiated DW cells [20].

In conclusion, photobiomodulation at a wavelength of 660 nm enhances gene expression of proteins involved in the ECM. The profile is dependent on the culture conditions and stressors placed on the cells. Increased glucose concentration in the culture media was associated with impaired gene regulation, which could be accountable for the poor response of these cells seen in wound healing. Previous studies have not exploited the role of LILI in gene expression of proteins in the ECM using fibroblast cells *in vitro*. This study was able to show the gene profile in normal and diabetic wound healing *in vitro*. The results also confirm the very important role exhibited by cell adhesion molecules (CAMs), integrins, ECM proteins, proteases, and inhibitors in wound healing. Therefore LILI mediated gene expression in wounded fibroblasts through paracrine and autocrine interactions to enhance wound healing. Further work on the molecular advances of gene modulation and their receptors will elucidate the therapeutic importance of LILI.

Disclosure

The material in this research paper has neither been published nor is being considered elsewhere for publication.

Conflict of Interests

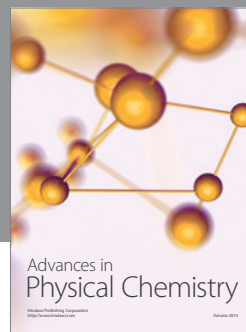
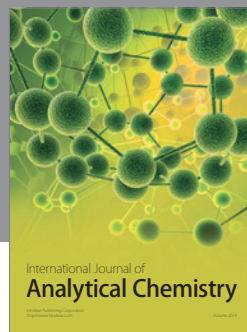
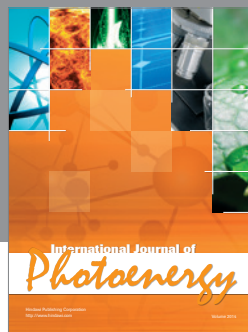
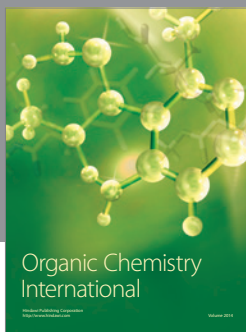
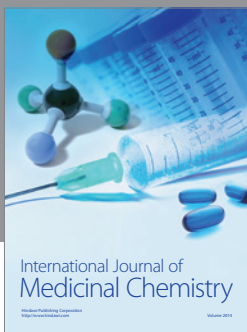
There is no conflict of interests regarding the publication of this paper.

References

- [1] M. S. Ågren and M. Werthén, "The extracellular matrix in wound healing: a closer look at therapeutics for chronic wounds," *International Journal of Lower Extremity Wounds*, vol. 6, no. 2, pp. 82–97, 2007.
- [2] G. S. Schultz, G. Ladwig, and A. Wysocki, "World wide wounds," 2005 <http://www.worldwidewounds.com/>.
- [3] M. S. Agren, W. H. Eaglstein, M. W. J. Ferguson et al., "Causes and effects of the chronic inflammation in venous leg ulcers," *Acta Dermato-Venereologica, Supplement*, no. 210, pp. 3–17, 2000.
- [4] S. F. Badyal, "The extracellular matrix as a scaffold for tissue reconstruction," *Seminars in Cell and Developmental Biology*, vol. 13, no. 5, pp. 377–383, 2002.
- [5] K. J. Rolfe and A. O. Grobbelaar, "The growth receptors and their role in wound healing," *Current Opinion in Investigational Drugs*, vol. 11, no. 11, pp. 1221–1228, 2010.
- [6] J. W. Penn, A. O. Grobbelaar, and K. J. Rolfe, "The role of the TGF-beta family in wound healing, burns and scarring a review," *International Journal of Burns and Trauma*, no. 1, pp. 18–28, 2012.
- [7] B. Eckes, R. Nischt, and T. Krieg, "Cell-matrix interactions in dermal repair and scarring," *Fibrogenesis and Tissue Repair*, vol. 3, no. 1, article 4, 2010.
- [8] W. P. Daley, S. B. Peters, and M. Larsen, "Extracellular matrix dynamics in development and regenerative medicine," *Journal of Cell Science*, vol. 121, no. 3, pp. 255–264, 2008.
- [9] J. J. Tomasek, G. Gabbiani, B. Hinz, C. Chaponnier, and R. A. Brown, "Myofibroblasts and mechano: regulation of connective tissue remodelling," *Nature Reviews Molecular Cell Biology*, vol. 3, no. 5, pp. 349–363, 2002.
- [10] D. J. Abraham, B. Eckes, V. Rajkumar, and T. Krieg, "New developments in fibroblast and myofibroblast biology: implications for fibrosis and scleroderma," *Current Rheumatology Reports*, vol. 9, no. 2, pp. 136–143, 2007.
- [11] E. G. Neilson, "Mechanisms of disease: Fibroblasts. A new look at an old problem," *Nature Clinical Practice Nephrology*, vol. 2, no. 2, pp. 101–108, 2006.
- [12] P. Price, K. Fogh, C. Glynn, D. L. Krasner, J. Osterbrink, and R. G. Sibbald, "Managing painful chronic wounds: the wound pain management model," *International Wound Journal*, vol. 4, supplement 1, pp. 4–15, 2007.
- [13] K. Soon and C. Acton, "Pain-induced stress: a barrier to wound healing," *Wounds*, vol. 2, no. 4, pp. 92–101, 2006.
- [14] S. Ryan, C. Eager, and R. G. Sibbald, "Venous leg ulcer pain," *Ostomy/Wound Management*, vol. 49, no. 4, supplement, pp. 16–23, 2003.
- [15] I. Anderson, "Aetiology, assessment and management of leg ulcers," *Wound Essentials*, vol. 1, pp. 20–36, 2006.
- [16] J. Kantor and D. J. Margolis, "Epidemiology: leg ulcers," in *A Problem-Based Learning Approach*, M. J. Morison, C. J. Moffatt, and P. J. Franks, Eds., pp. 65–73, Mosby, London, UK, 2007.
- [17] J. R. Mekkes, M. A. M. Loots, A. C. Van Der Wal, and J. D. Bos, "Causes, investigation and treatment of leg ulceration," *British Journal of Dermatology*, vol. 148, no. 3, pp. 388–401, 2003.
- [18] D. H. Evans and H. Abrahamse, "A review of laboratory-based methods to investigate second messengers in low-level laser therapy (LLLT)," *Medical Laser Application*, vol. 24, no. 3, pp. 201–215, 2009.
- [19] M. Simões Ribeiro, D. D. F. Teixeira Da Silva, C. E. Nabuco De Araújo et al., "Effects of low-intensity polarized visible laser radiation on skin burns: a light microscopy study," *Journal of Clinical Laser Medicine and Surgery*, vol. 22, no. 1, pp. 59–66, 2004.
- [20] S. M. Ayuk, N. N. Houreld, and H. Abrahamse, "Collagen production in diabetic wounded fibroblasts in response to low-intensity laser irradiation at 660 nm," *Diabetes Technology and Therapeutics*, vol. 14, no. 12, pp. 1110–1117, 2012.

- [21] R. Lubart, M. Eichler, R. Lavi, H. Friedman, and A. Shainberg, "Low-energy laser irradiation promotes cellular redox activity," *Photomedicine and Laser Surgery*, vol. 23, no. 1, pp. 3–9, 2005.
- [22] M. Eichler, R. Lavi, A. Shainberg, and R. Lubart, "Flavins are source of visible-light-induced free radical formation in cells," *Lasers in Surgery and Medicine*, vol. 37, no. 4, pp. 314–319, 2005.
- [23] K. Plaetzer, T. Kiesslich, B. Krammer, and P. Hammerl, "Characterization of the cell death modes and the associated changes in cellular energy supply in response to AlPcS4-PDT," *Photochemical and Photobiological Sciences*, vol. 1, no. 3, pp. 172–177, 2002.
- [24] P. V. Peplow, T.-Y. Chung, B. Ryan, and G. D. Baxter, "Laser photobiostimulation of wound healing: reciprocity of irradiance and exposure time on energy density for splinted wounds in diabetic mice," *Lasers in Surgery and Medicine*, vol. 43, no. 8, pp. 843–850, 2011.
- [25] H. Y. Chang, J.-T. Chi, S. Dudoit et al., "Diversity, topographic differentiation, and positional memory in human fibroblasts," *Proceedings of the National Academy of Sciences of the United States of America*, vol. 99, no. 20, pp. 12877–12882, 2002.
- [26] N. Hourelid and H. Abrahamse, "Irradiation with a 632.8 nm helium-neon laser with 5 J/cm² stimulates proliferation and expression of interleukin-6 in diabetic wounded fibroblast cells," *Diabetes Technology and Therapeutics*, vol. 9, no. 5, pp. 451–459, 2007.
- [27] G. Cory, "Scratch-wound assay," *Methods in Molecular Biology*, vol. 769, pp. 25–30, 2011.
- [28] K. P. Goetsch and C. U. Niesler, "Optimization of the scratch assay for in vitro skeletal muscle wound healing analysis," *Analytical Biochemistry*, vol. 411, no. 1, pp. 158–160, 2011.
- [29] G. S. Schultz and A. Wysocki, "Interactions between extracellular matrix and growth factors in wound healing," *Wound Repair and Regeneration*, vol. 17, no. 2, pp. 153–162, 2009.
- [30] K. S. Midwood, L. V. Williams, and J. E. Schwarzbauer, "Tissue repair and the dynamics of the extracellular matrix," *International Journal of Biochemistry and Cell Biology*, vol. 36, no. 6, pp. 1031–1037, 2004.
- [31] T. Okegawa, R.-C. Pong, Y. Li, and J.-T. Hsieh, "The role of cell adhesion molecule in cancer progression and its application in cancer therapy," *Acta Biochimica Polonica*, vol. 51, no. 2, pp. 445–457, 2004.
- [32] R. O. Hynes, "Integrins: bidirectional, allosteric signaling machines," *Cell*, vol. 110, no. 6, pp. 673–687, 2002.
- [33] T. Yagi and M. Takeichi, "Cadherin superfamily genes: functions, genomic organization, and neurologic diversity," *Genes and Development*, vol. 14, no. 10, pp. 1169–1180, 2000.
- [34] G. Maheshwari, G. Brown, D. A. Lauffenburger, A. Wells, and L. G. Griffith, "Cell adhesion and motility depend on nanoscale RGD clustering," *Journal of Cell Science*, vol. 113, no. 10, pp. 1677–1686, 2000.
- [35] R. L. Juliano, "Signal transduction by cell adhesion receptors and the cytoskeleton: functions of integrins, cadherins, selectins, and immunoglobulin-superfamily members," *Annual Review of Pharmacology and Toxicology*, vol. 42, pp. 283–323, 2002.
- [36] L. Petruzzelli, M. Takami, and H. D. Humes, "Structure and function of cell adhesion molecules," *The American Journal of Medicine*, vol. 106, no. 4, pp. 467–476, 1999.
- [37] J. Myllyharju and K. I. Kivirikko, "Collagens, modifying enzymes and their mutations in humans, flies and worms," *Trends in Genetics*, vol. 20, no. 1, pp. 33–43, 2004.
- [38] J. Sottile and D. C. Hocking, "Fibronectin polymerization regulates the composition and stability of extracellular matrix fibrils and cell-matrix adhesions," *Molecular Biology of the Cell*, vol. 13, no. 10, pp. 3546–3559, 2002.
- [39] T. Velling, J. Risteli, K. Wennerberg, D. F. Mosher, and S. Johansson, "Polymerization of type I and III collagens is dependent on fibronectin and enhanced by integrins $\alpha 1 \beta 1$ and $\alpha 2 \beta 1$," *Journal of Biological Chemistry*, vol. 277, no. 40, pp. 37377–37381, 2002.
- [40] K. E. Kadler, C. Baldock, J. Bella, and R. P. Boot-Handford, "Collagens at a glance," *Journal of Cell Science*, vol. 120, no. 12, pp. 1955–1958, 2007.
- [41] A. D. Bradshaw, D. C. Graves, K. Motamed, and E. H. Sage, "SPARC-null mice exhibit increased adiposity without significant differences in overall body weight," *Proceedings of the National Academy of Sciences of the United States of America*, vol. 100, no. 10, pp. 6045–6050, 2003.
- [42] M. Seux, S. Peugot, M. P. Montero et al., "TP53INP1 decreases pancreatic cancer cell migration by regulating SPARC expression," *Oncogene*, vol. 30, no. 27, pp. 3049–3061, 2011.
- [43] M. Koppen, M. D. Metodiev, G. Casari, E. I. Rugarli, and T. Langer, "Variable and tissue-specific subunit composition of mitochondrial m-AAA protease complexes linked to hereditary spastic paraplegia," *Molecular and Cellular Biology*, vol. 27, no. 2, pp. 758–767, 2007.
- [44] Z. Li, S. Guo, F. Yao, Y. Zhang, and T. Li, "Increased ratio of serum matrix metalloproteinase-9 against TIMP-1 predicts poor wound healing in diabetic foot ulcers," *Journal of Diabetes and Its Complications*, vol. 27, no. 4, pp. 380–382, 2013.
- [45] T. R. Kyriakides, D. Wulsin, E. A. Skokos et al., "Mice that lack matrix metalloproteinase-9 display delayed wound healing associated with delayed reepithelization and disordered collagen fibrillogenesis," *Matrix Biology*, vol. 28, no. 2, pp. 65–73, 2009.
- [46] V. Masson, L. Rodriguez De La Ballina, C. Munaut et al., "Contribution of host MMP-2 and MMP-9 to promote tumor vascularization and invasion of malignant keratinocytes," *The FASEB Journal*, vol. 19, no. 2, pp. 234–236, 2005.
- [47] G. Bix and R. V. Iozzo, "Matrix revolutions: 'Tails' of basement-membrane components with angiostatic functions," *Trends in Cell Biology*, vol. 15, no. 1, pp. 52–60, 2005.
- [48] Y. Hamano, M. Zeisberg, H. Sugimoto et al., "Physiological levels of tumstatin, a fragment of collagen IV $\alpha 3$ chain, are generated by MMP-9 proteolysis and suppress angiogenesis via $\alpha V \beta 3$ integrin," *Cancer Cell*, vol. 3, no. 6, pp. 589–601, 2003.
- [49] J. P. Hodde and C. E. Johnson, "Extracellular matrix as a strategy for treating chronic wounds," *The American Journal of Clinical Dermatology*, vol. 8, no. 2, pp. 61–66, 2007.
- [50] A. H. Hsieh, C. M.-H. Tsai, M. Qing-Jun et al., "Time-dependent increases in type-III collagen gene expression in medial collateral ligament fibroblasts under cyclic strains," *Journal of Orthopaedic Research*, vol. 18, no. 2, pp. 220–227, 2000.
- [51] R. P. Butt and J. E. Bishop, "Mechanical load enhances the stimulatory effect of serum growth factors on cardiac fibroblast procollagen synthesis," *Journal of Molecular and Cellular Cardiology*, vol. 29, no. 4, pp. 1141–1151, 1997.

- [52] M. Muller, C. Trocme, B. Lardy, F. Morel, S. Halimi, and P. Y. Benhamou, "Matrix metalloproteinases and diabetic foot ulcers: the ratio of MMP-1 to TIMP-1 is a predictor of wound healing," *Diabetic Medicine*, vol. 25, no. 4, pp. 419–426, 2008.
- [53] K. C. Ongenaes, T. J. Phillips, and H.-Y. Park, "Level of fibronectin mRNA is markedly increased in human chronic wounds," *Dermatologic Surgery*, vol. 26, no. 5, pp. 447–451, 2000.
- [54] R. Lobmann, C. Zemlin, M. Motzkau, K. Reschke, and H. Lehnert, "Expression of matrix metalloproteinases and growth factors in diabetic foot wounds treated with a protease absorbent dressing," *Journal of Diabetes and Its Complications*, vol. 20, no. 5, pp. 329–335, 2006.



Hindawi

Submit your manuscripts at
<http://www.hindawi.com>

